Multidimensional Tests of Thermal Protection Materials in the Arcjet Test Facility

Parul Agrawal*
ELORET Corporation, Sunnyvale, CA 94087

Donald T. Ellerby† , Mathew R. Switzer‡, Thomas H. Squire§
NASA Ames Research Center, Moffett Field, CA 94035-1000

Many thermal protection system materials used for spacecraft heatshields have anisotropic thermal properties, causing them to display significantly different thermal characteristics in different directions, when subjected to a heating environment during flight or arcjet tests. This paper investigates the effects of sidewall heating coupled with anisotropic thermal properties of thermal protection materials in the arcjet environment. Phenolic Impregnated Carbon Ablator (PICA) and LI-2200 materials (the insulation material of Shuttle tiles) were used for this study. First, conduction-based thermal response simulations were carried out, using the Marc.Mentat finite element solver, to study the effects of sidewall heating on PICA arcjet coupons. The simulation showed that sidewall heating plays a significant role in thermal response of these models. Arcjet tests at the Aerodynamic Heating Facility (AHF) at NASA Ames Research Center were performed later on instrumented coupons to obtain temperature history at sidewall and various radial locations. The details of instrumentation and experimental technique are the prime focus of this paper. The results obtained from testing confirmed that sidewall heating plays a significant role in thermal response of these models. The test results were later used to verify the two-dimensional ablation, thermal response, and sizing program, TITAN. The test data and model predictions were found to be in excellent agreement.

I. Introduction

Arcjet tests are performed to investigate the thermal response of TPS materials at very high heat flux and entry-like atmospheric pressure. The tests are conducted in the wind tunnel facilities that produce high enthalpy hypersonic flows, with the help of powerful arc heaters [1]. The tests are also used to provide experimental data to develop and validate thermal response modeling of TPS materials [2, 3]. The coupons used for the validation of thermal response models are usually axisymmetric, with an Iso-Q" shape, to provide uniform heat flux at the stagnation surface. They are instrumented with centerline thermocouples to measure temperature history during the high temperature plasma exposure and cooldown period afterwards. Optical pyrometers are also used to obtain the surface temperature at the stagnation point. To validate the response models, thermocouple and pyrometer data are compared against the numerically predicted thermal response. Historically, many the thermal response modeling approaches used for heatshield design and sizing are based on one-dimensional governing equations. Therefore, for

* Senior Research Scientist, NASA Ames Research Center, Thermal Protection Materials and Systems Branch, MS 234-1, Moffett Field, CA 94035, AIAA Member
† Materials Research Engineer, NASA Ames Research Center, Thermal Protection Materials and Systems Branch, MS 234-1, Moffett Field, Moffett Field, CA 94035
‡ Materials Engineer, NASA Ames Research Center, Thermal Protection Materials and Systems Branch, MS 242-6, Moffett Field, CA 94035
§ Aerospace Engineer, NASA Ames Research Center, Thermal Protection Materials and Systems Branch, MS 234-1, Moffett Field, CA 94035, AIAA Member

validation purposes, it is assumed that the centerline thermocouple data represents one-dimensional heating conditions [4]. However, the computational fluid dynamic predictions show that the cylindrical sidewall of an arcjet test coupon that is exposed to a heating environment could receive up to 10–13% of stagnation point heat flux [5]. If an anisotropic material has significantly different thermal conductivity in different directions through the material, the effects of sidewall heating become very prominent and the one-dimensional assumptions are not valid. Energy entering from the cylindrical surface of the sample may conduct more rapidly towards the center of the model than would the same amount of energy entering from the stagnation surface. Even for a short test, charring from sidewall heating becomes significant as shown in Figure 1. For materials like PICA, which is transverse isotropic with significantly higher conductivity "in-plane" than "thru-the-thickness", the one-dimensional response models usually underpredict the centerline temperature rise [5]. Therefore, it is important to investigate the extent of sidewall heating and its effects on the material coupons.

A parametric two-dimensional transient finite element analysis was performed on an idealized arcjet model exposed to sidewall heat flux along with the front surface heat flux. The model was based on pure thermal conduction and did not include pyrolysis or ablation. The purpose of these analyses was to assess the relative effect of sidewall heating on the temperature response at the centerline of the PICA sample. The details are provided in Section 2. Special tests were then designed and conducted at the Aerodynamic Heating Facility (AHF) at NASA Ames Arcjet Complex to assess the magnitude of sidewall heating and its effect on temperature history of the materials. The coupons were instrumented with thermocouples at various off-axis radial locations at different depths from the stagnation point. The facility description, design, and fabrication details of the test coupons are provided in the later sections of this paper.

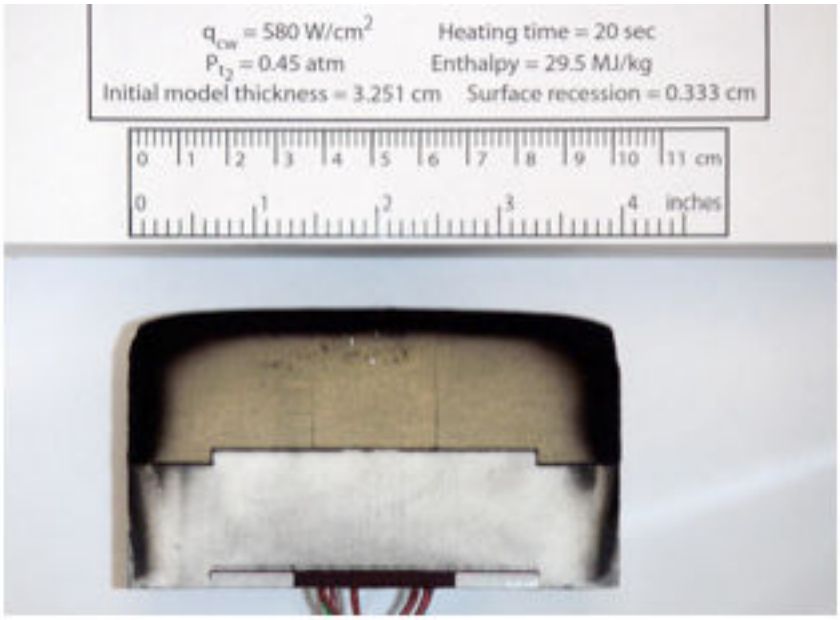

Figure 1. PICA coupon after arcjet test.

II. Analysis Model Development and Results

The finite element (FE) analyses were performed with the MSC.Marc commercial finite element package. MSC.Marc supports fully transient, non-linear, coupled thermal/mechanical FE analyses [6]. The model geometry is shown in Figure 2. It is axisymmetric with a 2 in (5.08cm) radius and is 3.683 in (9.36 cm) deep. The 4 in (10.16 cm) radius curvature on the forward face is meant to approximate an Iso-Q surface. That is, under arcjet heating conditions, the forward surface of the model should experience nearly uniform heat flux. This assumption will be used in the application of the heating boundary conditions. Only the PICA tile was included in the finite element analysis model. The back face of the sample, which would actually be attached to the test fixture, was assumed to be adiabatic. The finite element model took advantage of the axisymmetric nature of the geometry and heating conditions and was created using 2-D axisymmetric elements. The model was constructed of a mesh of 8-noded

quadrilateral elements with bi-quadratic interpolation functions. The axis of symmetry is along the X-coordinate. The model consisted of approximately 15000 nodes and 4900 elements. The thermal properties were based on recent measurements of PICA properties from the Crew Exploration Vehicle TPS Advanced Development Project (CEV TPS ADP)[7].

The measured thermal conductivity of PICA shows a strong directional dependence. In order to accommodate the expected temperature range in the analyses, the conductivity curves were extrapolated to temperatures higher than the material would be realistically expected to operate. Pyrolysis and ablation of PICA were not modeled in the conduction analyses. The purpose of the parametric analyses was to evaluate the relative influence of the sidewall heating on the thermal response of the model. The predicted temperatures at the stagnation point do not accurately represent the actual temperature during arcjet tests. A constant heat flux of 580 W/cm^2 (511 Btu/ft^2-s) was applied to the forward surface of the model. The heat flux at the rounded corner was assumed to vary linearly with stream length from the peak value to the sidewall value. The heat flux on the lateral sidewall of the model was varied parametrically as a percentage of the stagnation value, for 0%, 2%, 5%, and 10%. The forward surface, corner, and sidewall are also allowed to re-radiate to the environment, which is at a room temperature of 70 °F (294K). The back face of the model was adiabatic. The entire model was initially set to room temperature (294K, 70 °F). During the transient analyses, the heat flux was linearly increased from zero to the peak value over a period of one second. This "start up" period helps mitigate the transient artifacts in the solution. The total heating time was also varied parametrically for 15 seconds, 30 seconds, and 60 seconds. After the heat pulse, the model was allowed to cool down, through radiation to the environment, for 500 seconds.

The temperature history results at two centerline locations in the model were compared with one another. The two locations were 1 in (2.54 cm) and 2 in (5.08 cm) from the surface. Figure 3 and Figure 4 show the temperature history curves of the in-depth response for the 15- and 60-second heat exposure, respectively. Each figure includes the four different sidewall-heating levels. The 0% sidewall heating case would be closest to representing a pure 1-D conduction condition with energy entering the model only from the forward surface. The existence of the sidewall heating, even at 2% of the stagnation value, had a significant effect on the centerline thermal response at both in-depth locations for all heating conditions. For any given heating condition, the 2-D effect was most pronounced at the 2 in location. The sidewall heating not only increased the peak temperature at the in-depth locations, but it also shifted the time that the peak temperature occurred. Closer to the surface, at the 1 in depth location, the time-to-peak temperature increased as the sidewall heating increased. Further in depth, at the 2 in location, the time-to-peak temperature decreased as the sidewall heating increased. At the 1 in deep location, the effect of the sidewall heating was clearly apparent after about 100 seconds. At the 2" deep location, the effect was apparent after only about 50 seconds. In fact, at the 2 in location for the 15-second exposure, the rise in temperature was due as much to sidewall heating as to the stagnation surface heating, even for the 2% case. This supports the intuitive conclusion that the further in depth a point is, the more pronounced are the 2-D effects.

Figure 5 shows the temperature contours for the 15-second heating pulse case for all of the sidewall heating conditions: 0%, 2%, 5%, and 10%. The contours clearly show the large differences in temperature distributions that develop with increasing sidewall heating. Figure 6 shows the peak temperature at the two in-depth locations as a function of the sidewall heating. These analyses clearly show the relative effect of 2-D conduction on the thermal response at the centerline of a PICA arcjet model. The results indicate that for a 4in-diameter PICA arcjet model, centerline temperatures are influenced by multidimensional heat conduction from the sidewall at depths of about 1 inch or greater, or at times of about 100 seconds or greater. In general, the further in depth from the stagnation surface, the sooner the multidimensional effects become apparent and the larger they grow in magnitude. This study made a compelling case to investigate further and carry out the arcjet tests to measure the sidewall temperature and obtain off-axis thermal response for PICA coupons. The next few sections describe the model fabrication and arcjet test results.

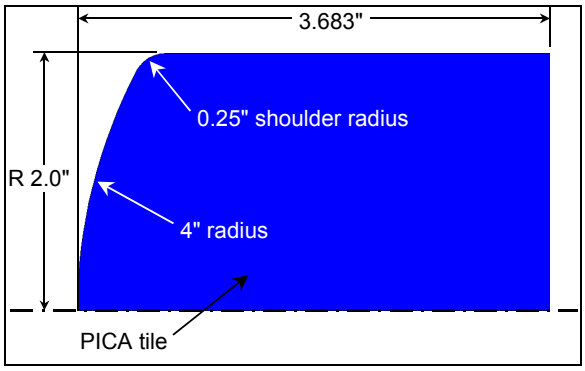

Figure 2. Arcjet model geometry for finite element analysis.

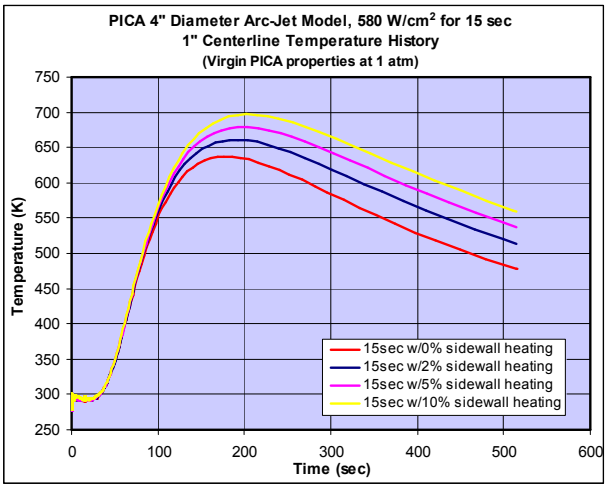

a) 1 in depth

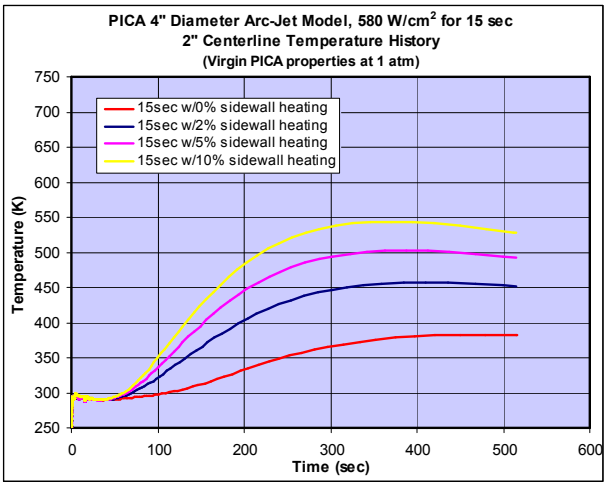

b) 2 in depth

Figure 3. In-depth temperature history for 15-second heat pulse.

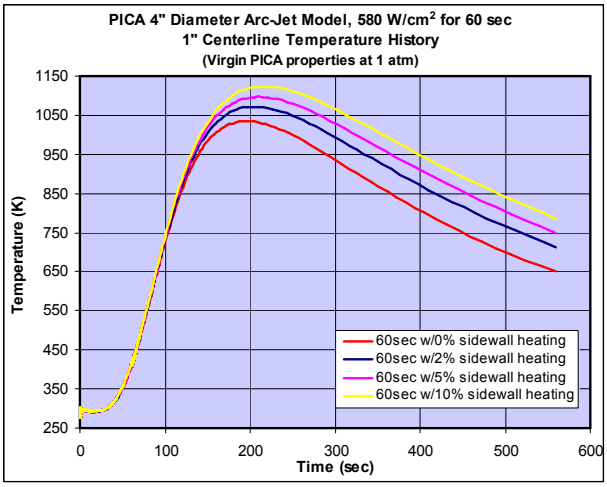

a) 1 in depth

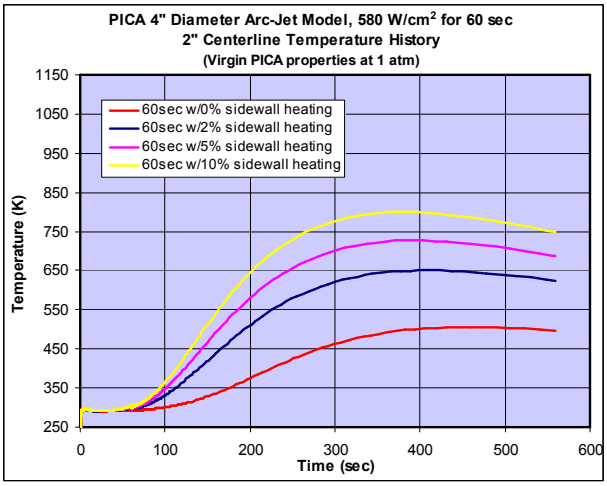

b) 2 in depth

Figure 4. In-depth temperature history for 60 second heat pulse.

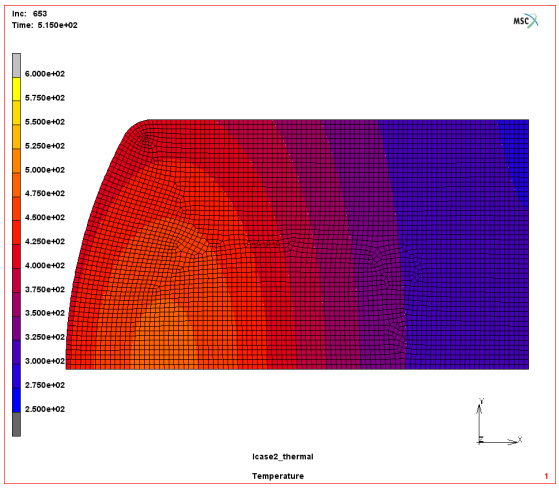

a) 0% sidewall heating

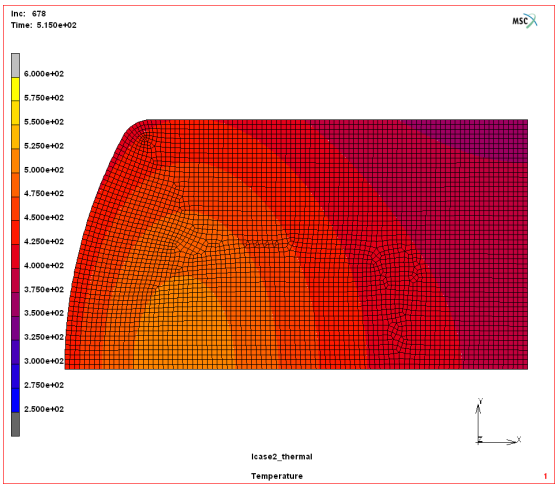

b) 2% sidewall heating

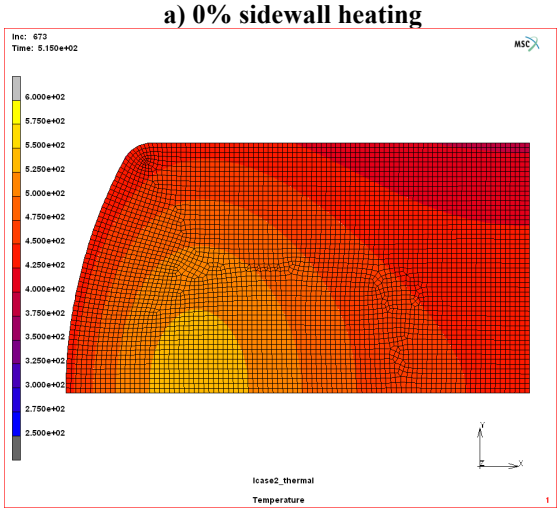

c) 5% sidewall heating

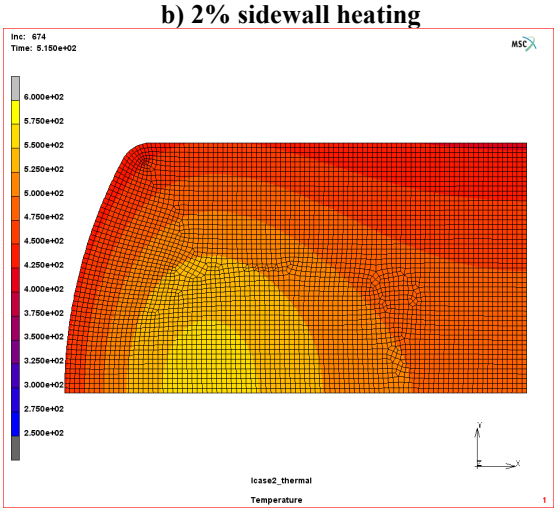

d) 10% sidewall heating

Figure 5. Temperature contours (K) at 515 seconds.

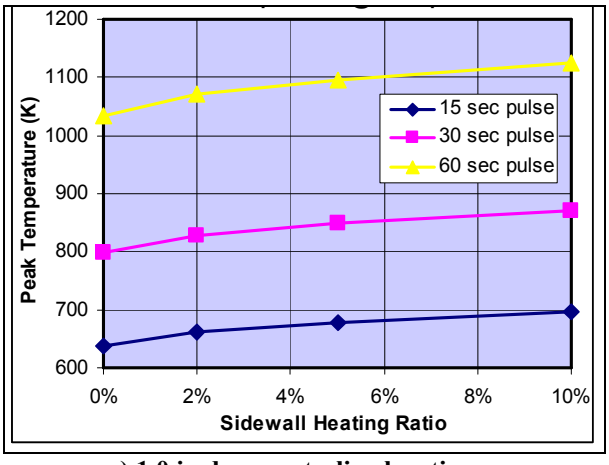

a) 1.0 in deep centerline location

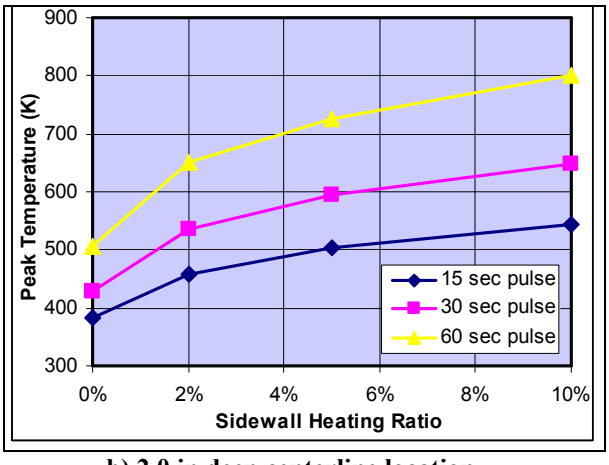

b) 2.0 in deep centerline location

Figure 6. Peak in-depth temperature vs. sidewall heating

III. Test Article Design, Fabrication, and Instrumentation

The FEA results showed that sidewall heating could significantly affect the thermal response of the coupons even at the centerline. We decided to investigate this phenomenon further and conduct the arcjet runs on coupons that would be instrumented with thermocouples at the sidewall and other radial locations at various depths. There were two types of test articles planned for this run. The first category consisted of PICA samples with centerline and off-axis thermocouples at various depths. These coupons were used for validation of the multidimensional thermal response model. Standard PICA coupons with centerline thermocouples only served as a control for comparison to the temperature history of centerline thermocouples from PICA coupons that had off-axis thermocouples along with centerline thermocouples. The second category of samples was made of LI-2200 material with thermocouples on the stagnation point and at various heights from the stagnation point at the sidewall surface. These coupons were used to obtain temperature history at various locations on the cylindrical sidewall in order to validate the CFD predictions of sidewall heating. A summary of all the test articles is provided in

Table **1**.

A. PICA Coupons Dimensions and Model Design

A novel design and instrumentation approach was developed at NASA Ames Research Center to fabricate the PICA test coupons with embedded off-axis and centerline thermocouples. The model was fabricated with internal lobes containing the off-axis thermocouples, centerline plug and the LI-2200 holder at the base. The overall coupon height at the stagnation point was 1.625 inches (4.128 cm) and diameter was 4.0 inches (10.16 cm). The front stagnation face was designed and cut according to the Iso-Q geometry to ensure uniform heat flux. The off-axis thermocouples were installed using a three-lobed cloverleaf-shaped architecture encapsulating the centerline plug. These lobes were fabricated to provide different radial locations away from centerline. Two of these cloverleaf insert were laid on top of each other and inserted on the outer PICA shell. The lobes were separated by 120° angle. The lobes on the top insert were of different size, so that thermocouples could be mounted at different radial locations. On the bottom insert, all three lobes were of same size, positioning all thermocouples at the same radius to be separated by a 120° angle. The objective behind this design was to investigate the azimuthal symmetry of heat flux and temperature distributions. The analysis results showed that at the farthest distance from the center stagnation point, the effects of sidewall heating are more pronounced. Therefore, the lobes were design to provide significant distance between the center stagnation point and the off-axis thermocouple. A cylindrical plug, embedded with thermocouples along the centerline at different locations, was inserted through the center of the inserts. Both the centerline cylindrical plug and three-lobed inserts were made of PICA. A LI-2200 holder was bonded to the base of the model.

The assembly sequence and picture of the model are shown in Figure 7 and Figure 8. X-ray scans were taken for all the coupons to ensure correct thermocouple installation and to allow accurate measurement of their locations inside each coupon. The top and side views of X-ray images of the coupon, showing various thermocouple locations, are shown in Figure 9 A and B**,** respectively. It can be clearly seen from the images that the thermocouples were azimuthally equidistant. Figure 10 shows the map of thermocouples (TC) for these samples. Nominal thermocouple locations and their types are listed in Table 2.

PICA coupons, instrumented only with centerline thermocouple plugs, were used as controls for this test series. The locations of thermocouples on control PICA coupons are also listed in Table 2. These coupons were fabricated at Boeing. The thickness for control coupons at the stagnation point was 1.375 inch.

B. LI-2200 Coupon Dimensions and Model Design

The LI-2200 samples were designed to get an accurate surface temperature measurement from the front face and sidewall. The objective was to obtain sidewall heating rates for comparison with CFD predictions. These coupons were also 4.0 inches (10.16 cm) in diameter with an Iso-Q shape at the front face. The overall height of the model including the holder was 4.0 inches (10.16 cm). The samples and holders were made of LI-2200. The model height, without the holder, was 2.0 inches (5.08 cm). These samples were coated with Reaction-Cured Glass (RCG) on the top and at the sidewall to restrain the flow of hot gases inside LI-2200 coupons and provide higher emissivity for radiation equilibrium. Thermocouples were embedded below the surface coating. There was one thermocouple mounted at the stagnation point and the other five thermocouples were located at the sidewall surface at different

distances from the stagnation point. Figure 11 shows X-ray scans of the sample with embedded thermocouples. The actual depths and radial locations of these thermocouples are listed in Table 2.

Table 1. Description of test articles

Material	Objective	Diameter & OML	Coupons thickness at the stag area, inch	Coating	Model Instrumentation (Themocouples)
PICA	Thermal Response Model, control	4 inch Iso-Q	1.375	No	2 R-type, 3 K-type
PICA	Thermal Response Model, off-axis measurements	4 inch Iso-Q	1.625	No	1 R-type, 8 K-type
LI-2200	CFD validation, sidewall heating	4 inch Iso-Q	2.0	RCG	6 R-type

Table 2. Thermocouple depths and radial locations for test models

Model Type		TC1	TC2	TC3	TC4	TC5	TC6	TC7	TC8	TC9
	Depth from Stagnation point (inches)	0.15	0.30	0.45	0.60	1.20	N/A	N/A	N/A	N/A
PICA Control	Radial length from center (inches)	0.0	0.0	0.0	0.0	0.0	N/A	N/A	N/A	N/A
PICA Off-axis	Depth from Stagnation point (inches)	0.30	0.90	1.20	0.90	0.90	0.90	1.20	1.20	1.20
PICA Off-axis PICA Off-axis	Radial length from center (inches)	0.00	0.00	0.00	1.75	1.50	1.00	1.75	1.75	1.75
	Depth from Stagnation point (inches)	0.0	0.638	0.90	1.20	1.50	1.2(on sidewall 180 deg from TC-4)	N/A	N/A	N/A
LI-2200	Radial length from center (inches)	0.0	2.000	2.00	2.00	2.00	2.00	N/A	N/A	N/A

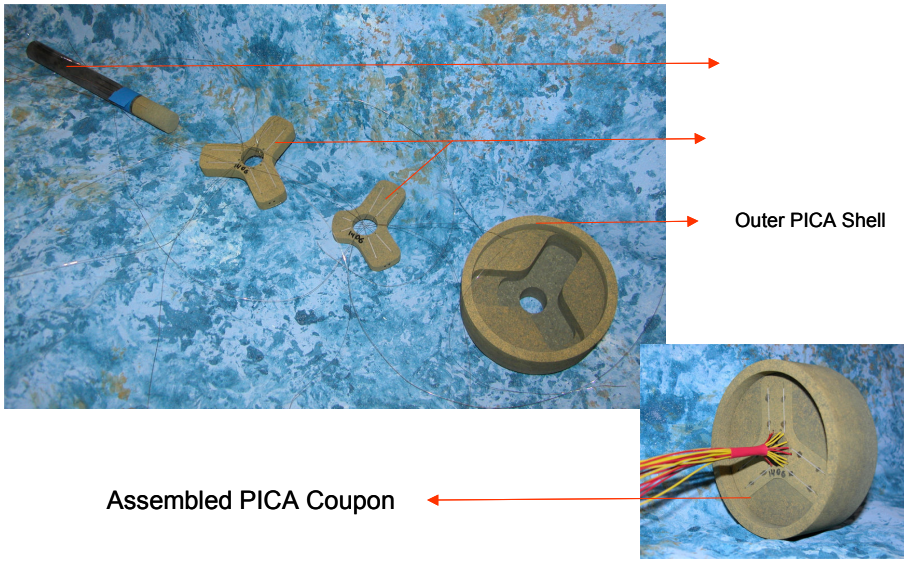

Figure 7. Assembly sequence of off-axis PICA coupons

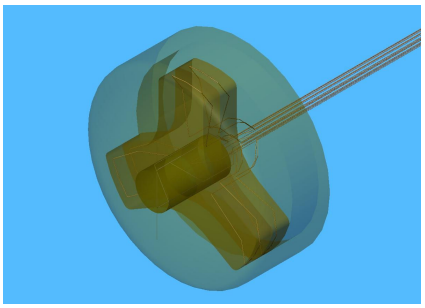

Figure 8. Drawing of PICS coupon showing the lobes and centerline plugs inserted inside the outer shell.

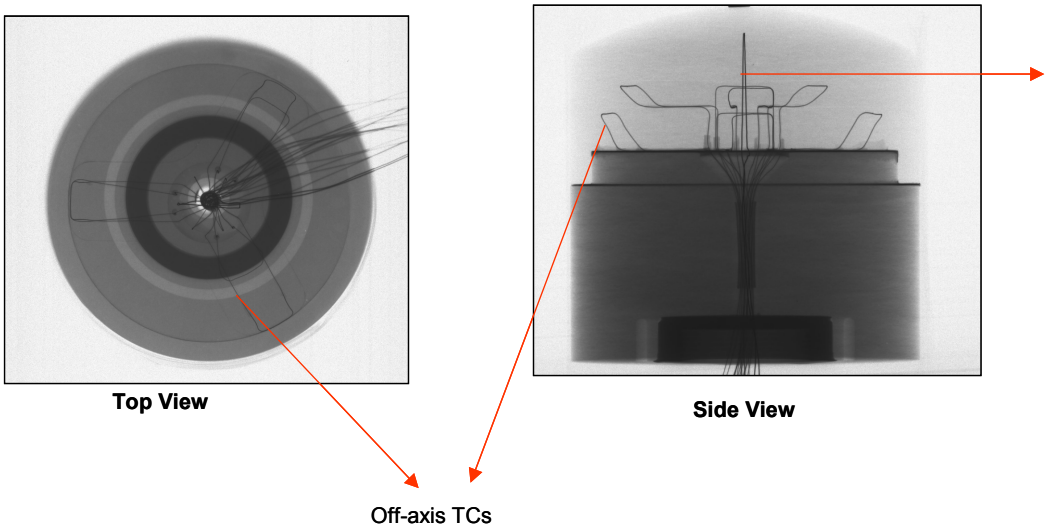

Figure 9. X-ray image of Off-axis PICA Coupons

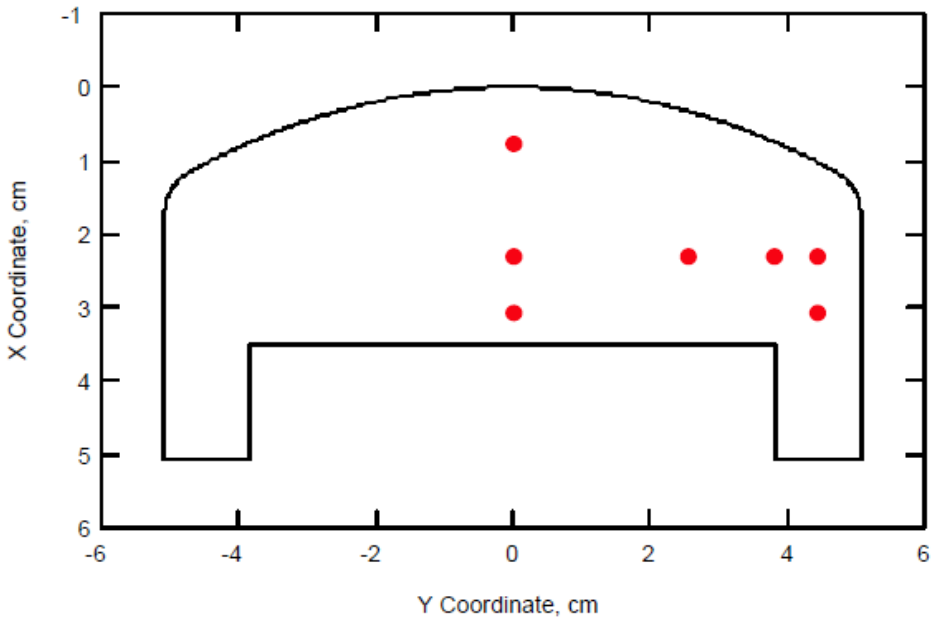

Figure 10. Thermocouple map for off-axis PICA coupons

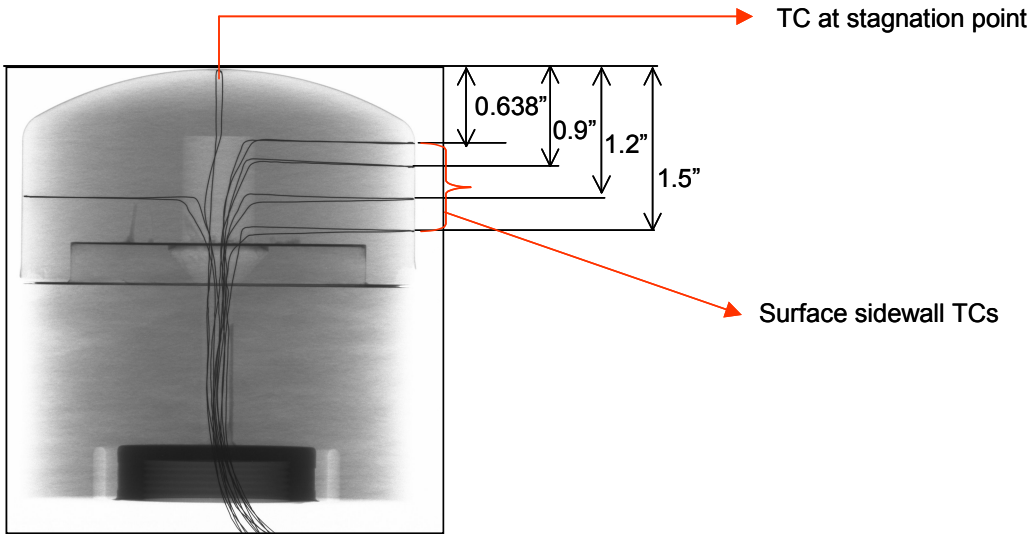

Figure 11. X-ray image of LI-2200 Coupon

IV. Test facility and Environment Description

The tests were conducted at the Aerodynamic Heating Facility (AHF) located at NASA Ames Research Center. It is a flexible arcjet facility that operates with 20-megawatt arc heaters and conical nozzles. The arc heater operates at pressures from 1.0 to 10.0 atm and enthalpy levels from 11.0 MJ/Kg to 32.0 MJ/Kg. The detailed description of the facility is provided in [2,3,8]. For these tests the arc heater was coupled with a conical nozzle of 8° half angle and 18.0 inch exit diameter. The nozzle was discharged into an 8 ft x 8 ft. x 8 ft. walk-in test chamber. Chamber pressure was a function of mass flow and pumping rates, ranging from 0.1 to 10 torr. Samples were mounted on a carriage arm consisting of five stings. Each sting could carry one sample. There was also a swing arm for slug calorimeter measurements. The samples were exposed to the plasma in an open jet, formed between the nozzle exit and the entrance to the diffuser. Figure **12** shows the coupons mounted inside the test chamber. The thermocouple extensions were routed to a patch panel inside the chamber for data recording. For optical pyrometers, as well as imaging, there were ports on the sides and ceiling of the test chambers. This allowed video recording of the test articles and the plasma streams.

Two different conditions were selected after studying the AHF performance envelope and past run histories. The low heat flux conditions were chosen, as LI-2200 coupons may not survive the heat flux beyond 250 W/cm^2, and it was essential to obtain the temperature at the sidewalls. The test durations corresponding to 175 W/cm^2 and 250 W/cm^2 conditions were chosen to maintain identical heat loads. Table 3 summarizes the run conditions and test matrix for each condition. For each condition, one calibration run was made with calorimeters of same dimensions as models. During each calibration run a Teflon sample was also exposed to the plasma stream, with a similar exposure as the LI-2200 and PICA coupons, to ensure the flow uniformity. After reviewing the calibration runs, the models were tested in subsequent runs. Each of these runs had one LI-2200 with surface-mount thermocouples, to study the sidewall heat flux, one standard PICA sample, with only centerline thermocouples, to serve as controls, and two PICA samples with embedded off-axis thermocouples at different depths and radial locations. Besides thermocouples, the data from optical pyrometers were also obtained for stagnation point and sidewall surface temperatures. The next section describes the test results and analytical model validation.

Table 3. Test Environment and Coupon Description

Run #	Condition	Cold Wall Heat Flux (W/cm2)	Pressure (KPa)	Stagnation Enthalpy (MJ/Kg)	Sample Material	Model ID	Exposure (sec)
1 (Calibration)	1	174	5.03	18.16	3.0" Hemi slug Calorimeter		
					4" ISO-Q Calorimeter		
					4" ISO-Q Calorimeter		
					4" ISO-Q Teflon	TT-0001	60
2 (Calibration)	2	246	8.48	20.05	3.0" Hemi slug Calorimeter		
					4" ISO-Q Calorimeter		
					4" ISO-Q Calorimeter		
					4" ISO-Q Teflon	TT-0002	42
3	1	175	5.07	18.24	3.0" Hemi slug Calorimeter		
					4" ISO-Q Calorimeter		
					PICA -HRL4.3 build-Control	AA-43-208-N	60
					LI-2200 (Sidewall TCs)	1401	60
					Off-axis PICA	1403	60
					Off-axis PICA	1404	60
4	2	248	8.48	20.18	3.0" Hemi slug Calorimeter		
					4" ISO-Q Calorimeter		
					PICA -HRL4.3 build-Control	AA-43-207-N	42
					LI-2200 (Sidewall TCs)	1402	42
					Off-axis PICA	1405	42
					Off-axis PICA	1406	42

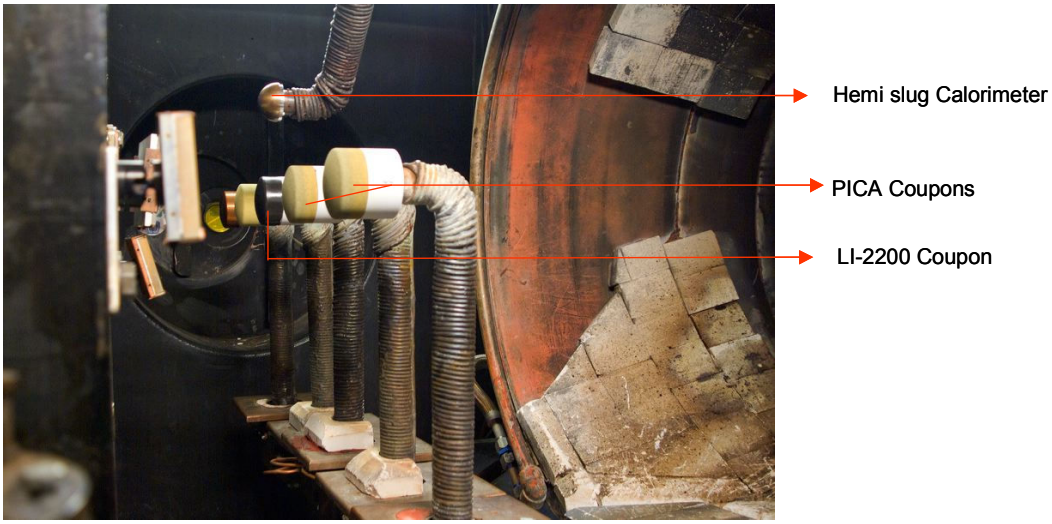

Figure 12. Coupons mounted inside the arcjet test chamber

V. Test Results and Analysis

The tests were successfully conducted, and we were able to achieve the target heat flux and pressure conditions. LI-2200 coupons with sidewall thermocouples survived heat flux at both temperatures, and no melting or significant distortion of the coupons was observed during the test. Figure shows the images of one of the LI-2200 coupons before, during, and after the test. From the thermocouple data, it was clear that the RCG coating protected the thermocouples and the coupons. This was an important test, because, for the first time during the arcjet tests, we recorded temperature history at the sidewall, to understand the extent of sidewall heating and help in analytical

model validation. Figure **14** shows the temperature history obtained from thermocouples and pyrometers on LI-2200 coupons. For the test run at 175 W/cm^2 heat flux, the maximum temperature at the stagnation point reached 1600 °C. Both pyrometer and stagnation point thermocouples showed the same value. The shoulder and sidewall thermocouples showed the temperature rise in the range of 700 °C–9000 °C. As expected, the closer the thermocouple depth was to the stagnation surface, the higher the temperature was achieved, with the shoulder thermocouple showing the highest value. The sidewall pyrometer showed a temperature rise to 650 °C. Due to a large imaging spot size of the pyrometer (1.0 inch diameter), it was hard to define the exact height the data corresponded to. For test run # 4, the temperature rise up to 1700 °C was recorded by the stagnation point thermocouple. At that point, the thermocouple reached its limit and stopped functioning. Pyrometer data at the stagnation point shows the steady maximum temperature of 1700 °C at the stagnation surface for the entire heat flux duration. The sidewall and shoulder thermocouples show the temperature rise in the range of 900–1000 °C, respectively. The data reaffirms that there is significant heating at the sidewall and multidimensional effects are significant**.** Figure **15** shows the comparison of thermocouple data at the stagnation surface and at the sidewall with CFD program prediction DPLR [9] and 2D thermal response code TITAN [10]. While, analytical predictions are in good agreement with thermocouple data at the stagnation point, they overpredict the temperature at and near the shoulder region. Further investigations are required to explain the discrepancy.

All the PICA coupons with off-axis and centerline thermocouple plugs also survived the test. No model disintegration or flow of hot gases through the sample was observed during the test. Images of one PICA model instrumented with off-axis thermocouples before, during, and after test run # 4 are shown in Figure **16**. It is clear from the post-test pictures that PICA coupons charred and recessed during the test. Laser scans and dial gauge measurements were performed on the samples to obtain the magnitude of recession and the post-test contours of recessed surfaces. The measurements confirmed that the presence of the off-axis thermocouples and different architecture of the coupons did not affect the overall coupon geometry and the test outcome.

The thermocouple data obtained during this test is shown in Figure 17 and Figure 18. The temperature rise corresponding to 175 W/cm^2 heat flux is shown in Figure , a and b. At 0.9 in" height from the stagnation point, the centerline thermocouple shows the temperature rise of 350 °C, whereas the thermocouple closest to the sidewall (at centerline radius of 1.75 in) shows the temperature rise of 950 °C. This is a very significant effect of sidewall heating, coupled with high in-plane conductivity of PICA. Figure 17a also shows that at 0.9 inch height, as we follow the radius away from the centerline, the temperature is steadily increasing. The thermocouple data is very consistent for both off-axis coupons. Figure b shows the comparison of temperature rise between centerline and 1.75in radial location at 1.2 inches height. The data from three different thermocouples, at 120° angles apart, are very consistent with each other and confirms the azimuthal symmetry of heat load entering into the coupons. The centerline thermocouple shows the temperature rise of 300 °C, whereas the off-axis thermocouples at 1.75 inches shows that they reached 700 °C at the peak value. The analytical predictions from TITAN and comparison to the test data are shown in

Figure 18 [5]. The TITAN predictions are in excellent agreement with the test data. The thermocouple data obtained from run # 4 (250 W/cm^2 flux) is shown in Figure 19 a and 19b. The data shows similar trend as the previous test run. The temperature rise at the sidewall thermocouples far exceeds the temperature rise at the centerline. Another interesting observation was that even though the heat loads for the two test conditions were very similar, the temperature rise at the centerline is about 50–100 °C lower for run # 4. However, the sidewall thermocouples show a very similar rise of temperature for both test conditions. The comparison with TITAN data for run # 4 is shown in Figure . Again, TITAN predictions are in excellent agreement with test data. Figure 21 shows the recession profile. The coupons maintained the ISO-Q shape during the test.

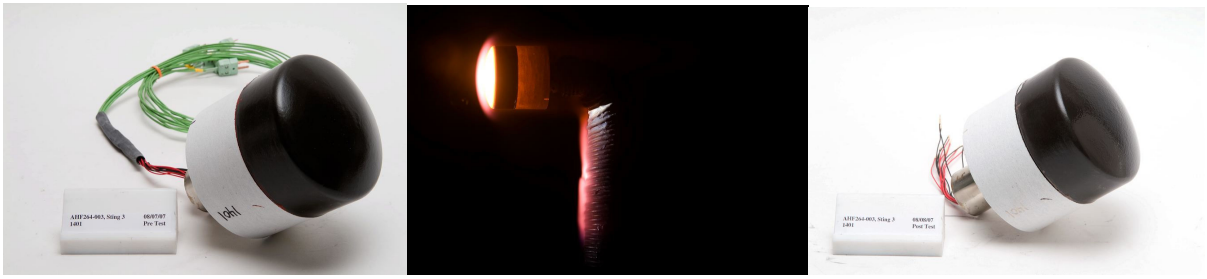

Figure 13. RCG coated LI-2200 coupons before, during and after arcjet test.

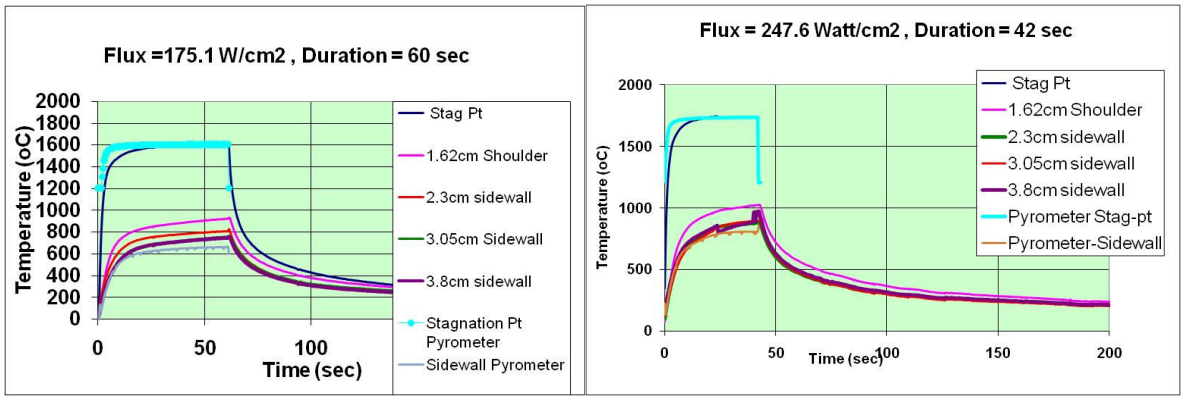

Figure 14. Temperature profile measured on LI-2200 Coupons, a) Run# 3 b) Run # 4

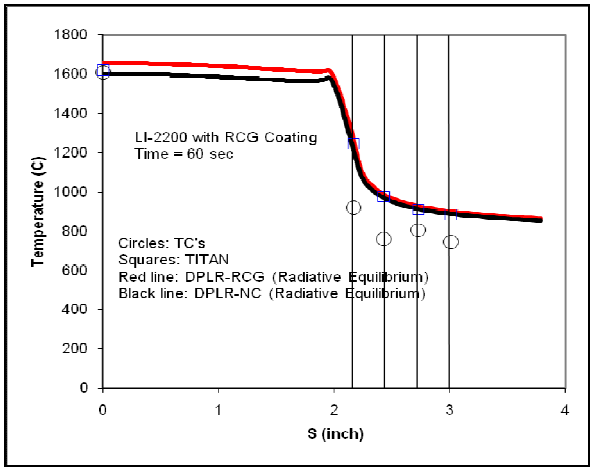

Figure 15.Comparison of sidewall thermocouple data in LI-2200 coupon with analytical models.

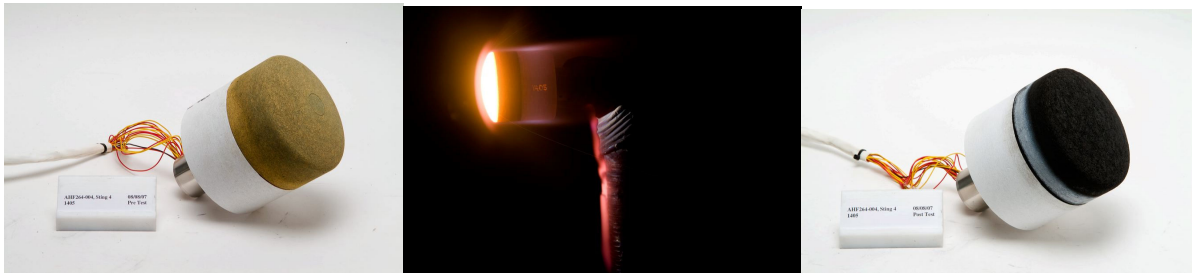

Figure 16. PICA coupon with off-axis thermocouple, before, during and after the arcjet test.

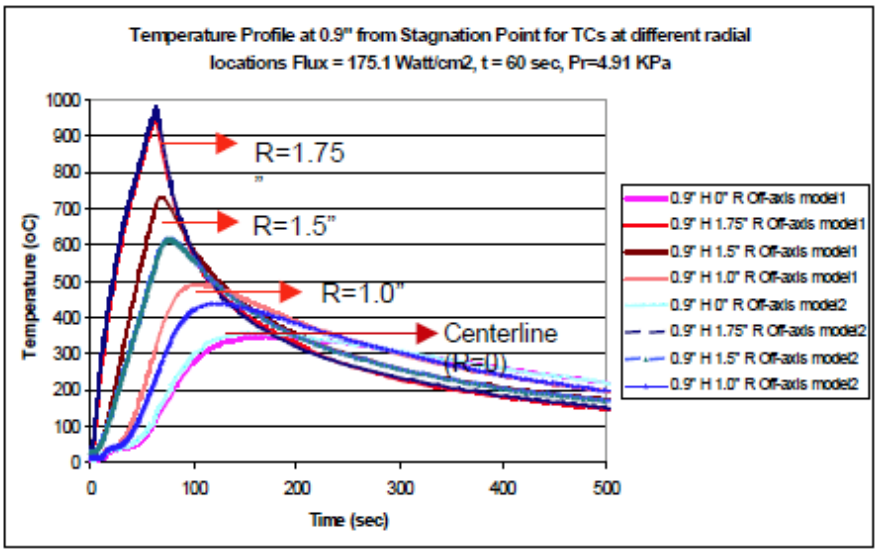

Figure 17a. Temperature profile measured on PICA Coupons for Run # 3 at 0.9in depth.

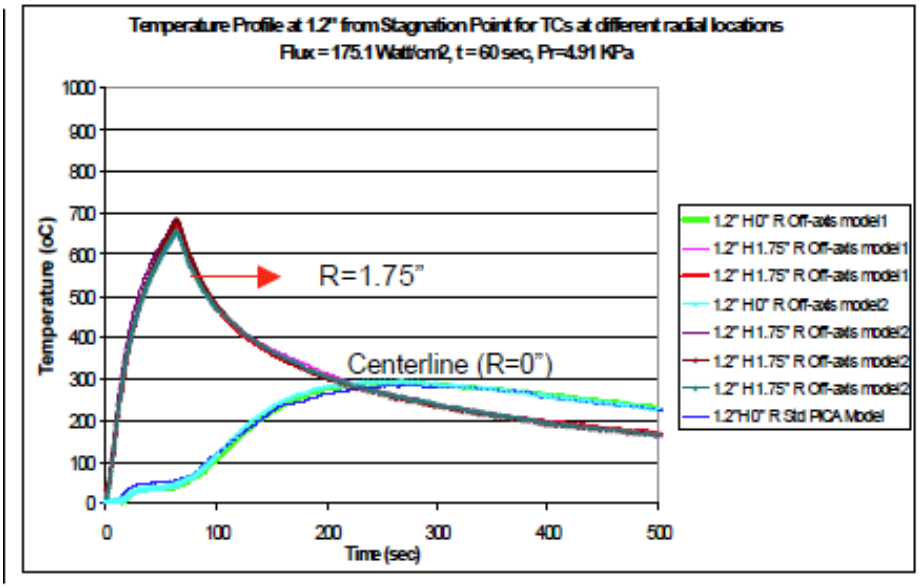

Figure 17b. Temperature profile measured on PICA Coupons for Run # 3 at 1.2in depth.

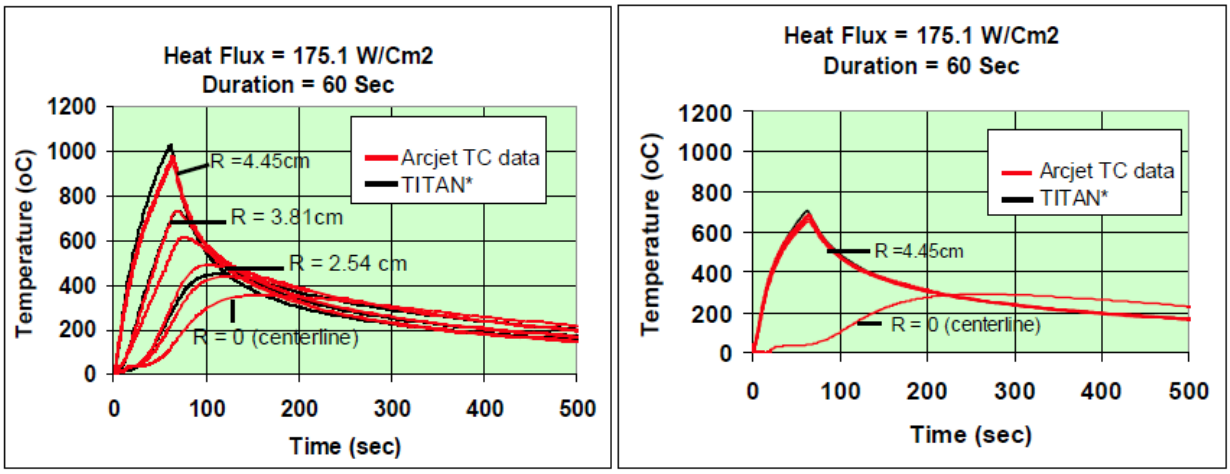

Figure 18. Comparison of thermocouple data with TITAN predictions for Run # 3

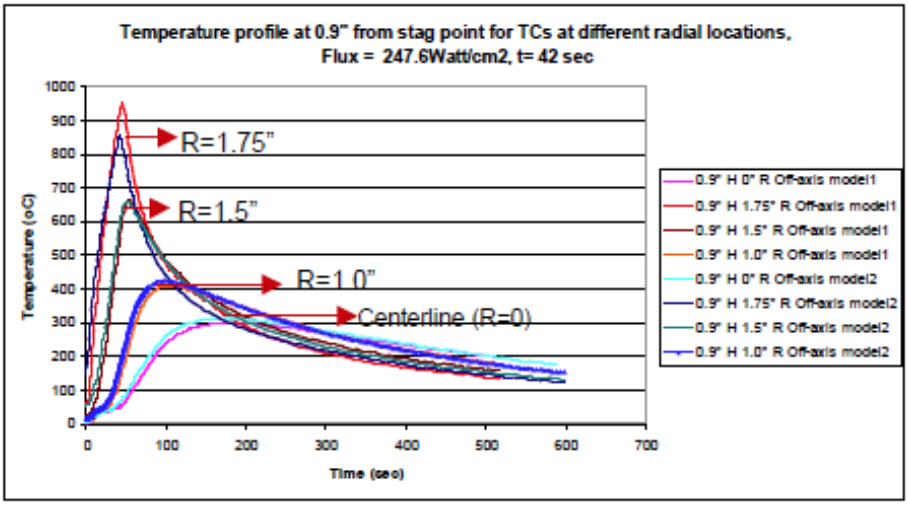

Figure 19a. Temperature profile measured on PICA Coupons for Run # 4 at 0.9in depth.

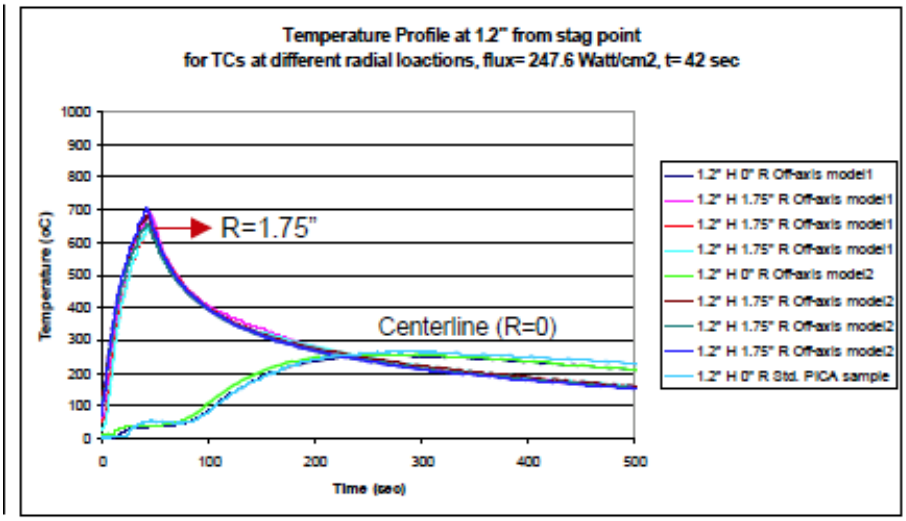

Figure 19b. Temperature profile measured on PICA Coupons for Run # 4 at 1.2 in depth.

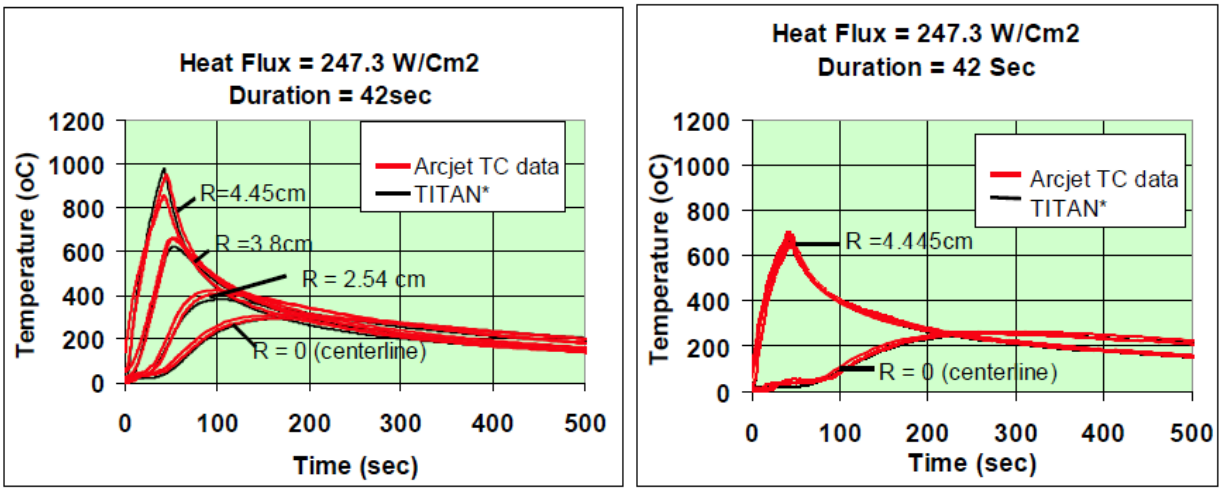

Figure 20. Temperature profile measured on PICA Coupons for Run # 4.

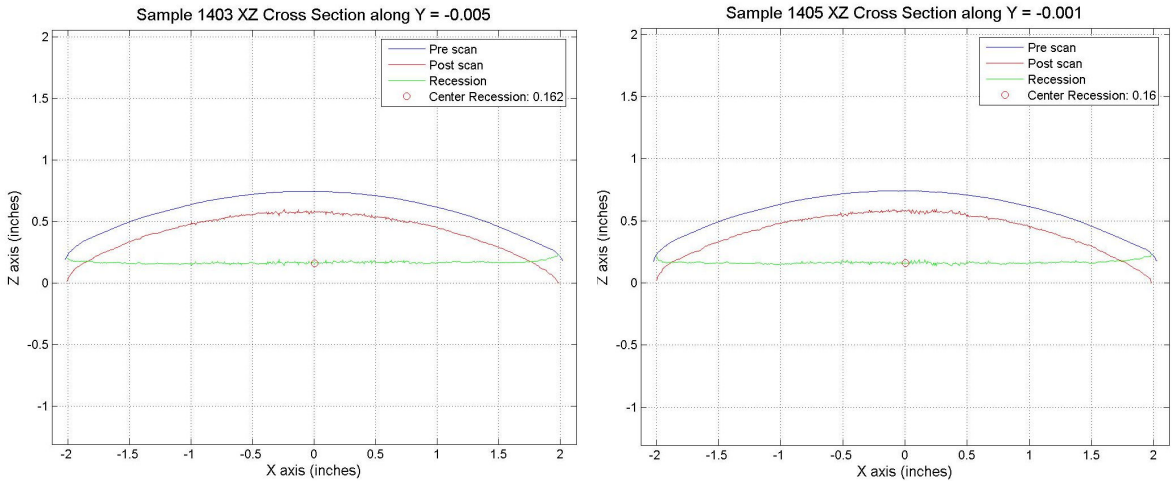

Figure 21. Pre and Post test laser scans to measure stagnation surface recession on PICA coupons.

VI. Conclusions

The effects of sidewall heating on PICA were successfully demonstrated, first through the analytical model, followed by arcjet testing. The authors were able to design and fabricate test articles that were instrumented with sidewall and off-axis thermocouples. The test runs were conducted at the Aerodynamic Heating Facility at NASA Ames Research Center. Both PICA and LI-2200 coupons with off-axis thermocouples survived the tests and temperature histories at various radial locations were obtained during the tests. The data showed that sidewall heating is significant during the arcjet tests and there is a very high temperature rise due to the sidewall heating when coupled with high in-plane conductivity. The data were later used to compare and validate two-dimensional thermal response code TITAN, developed by scientists at NASA Ames Research Center.

VII. Acknowledgment

The authors gratefully acknowledge the support provided by the Orion TPS Advanced Development Project specially Ethiraj Venkatapathy and NASA Ames Research Center through their contract to the ELORET Corporation. We also acknowledge the arcjet test facility engineer Frank Hui and NASA-SCAP for their critical financial support of the arcjet operational capability at NASA Ames Research Center.

VIII. References

[1] Peterson, A. B., Nichols, F., Mifsud, B., and Love,W., "Arc Jet Testing in NASA Ames Research Center Thermophysics Facilities," *AIAA paper 92-5041,* Dec. 1992.

[2]Laub, B., Balboni, J. and Goldstein, H., "Ground Test Facilities for TPS Development," NASA TM-2002-211400, NASA Ames Research Center, Moffett Field, California, May 2002.

[3]Laub, B., "Use of Arc-Jet Facilities in the Design and Development of Thermal Protection Systems", AIAA Paper 2006-3292**,** 25th AIAA Aerodynamic Measurement Technology and Ground Testing Conference, 5 - 8 June 2006, San Francisco, California.

[4] Chen, Y.-K. and Milos, F.S., "Ablation and Thermal Response Program for Spacecraft Heatshield Analysis," Paper 98-0273, AIAA 36th Aerospace Sciences Meeting & Exhibit, Reno, NV, Jan. 12-15, 1998.

[5]Milos, F.S. and Chen, Y.-K., "Ablation and Thermal Response Property Model Validation for Phenolic Impregnated Carbon Ablator", AIAA paper 2009-262, 47th AIAA Aerospace Sciences Meeting Including The New Horizons Forum and Aerospace Exposition, January 2009, Orlando, Florida.

[6] Anon., "MSC.Marc User Guide Version 2007".

[7] Milos, F.S., and Chen, Y.-K., "Ablation and Thermal Property Model for Phenolic Impregnated Carbon Ablator (PICA)," NASA/TM-2009-215377, Jan. 2009.

[8] Terrazas-Salinas, I., and Cornelison, C., "Test Planning Guide for ASF Facilities," Thermophysics Facilities Branch, Space Technology Division, NASA Ames Research Center, March 1999.

[9]Wright M.J., Candler,G.V. and Bose D. "Data-Parallel Line Relaxation Method for the Navier–Stokes Equations" AIAA Journal, Vol. 36, No. 9, 1603-1609.

[10]Milos, F.S. and Chen, Y.-K., "Two-Dimensional Ablation, Thermal Response, and Sizing Program for Pyrolyzing Ablators," AIAA Paper 2008-1223, AIAA Aerospace Sciences Meeting and Exhibition, January 2008.